Electronic Supplementary Information

Highly enhanced UV-vis-NIR light harvesting and photoelectric conversion of pyrene MOF by encapsulation of D-π-A cyanine dye

Xiao-Gang Yang,[a] Jian-Hua Qin,*[a] Ya-Dan Huang,[a] Zhi-Min Zhai,[a] Lu-Fang Ma,*[a] Dongpeng Yan*[b]

[a]College of Chemistry and Chemical Engineering, Luoyang Normal University, Henan Province Function-Oriented Porous Materials Key Laboratory, Luoyang 471934, China. E-mail: mazhuxp@126.com.

[b]College of Chemistry, Beijing Normal University, Beijing Key Laboratory of Energy Conversion and Storage Materials, Beijing 100875, China. E-mail: yandp@bnu.edu.cn.

*Corresponding author. E-mail: yandp@bnu.edu.cn; mazhuxp@126.com; jh_q128105@126.com

A. Experimental Section

1. Materials and general procedures.

All reagents were of analytical grade and obtained from commercial sources without further purification. Powder X-ray diffraction analyses (PXRD) patterns were collected on a Bruker D8-ADVANCE X-ray diffractometer with Cu *Kα* radiation (λ = 1.5418 Å). Measurements were made in a 2θ range of 5−50° at room temperature with a step of 0.02° (2*θ*) and a counting time of 0.2 s/ step. The operating power was 40 KV, 30 mA. Thermogravimetric analysis (TGA) experiments were carried out using SII EXStar6000 TG/DTA6300 thermal analyzer from room temperature to 800 ^{o}C under a nitrogen atmosphere at a heating rate of 10 ^{o}C min^{-1}.

Single-crystal X-ray diffraction data for **1** was collected at room temperature on an Oxford Diffraction SuperNova area-detector diffractometer using mirror optics monochromated Mo Kα radiation (λ = 0.71073 Å). CrysAlisPro[1] was used for the data collection, data reduction and empirical absorption correction. The crystal structure was solved by direct methods, using SHELXS-2014 and least-squares refined with SHELXL-2014[2] using anisotropic thermal displacement parameters for all non-hydrogen atoms. The crystallographic data for **1** are listed in Table S1 and S2. CCDC No. 1998196 contain the supplementary crystallographic data for **1**. This material can be obtained free of charge via http://www.ccdc.cam.ac.uk/conts/retrieving.html, or from the Cambridge Crystallographic Data Centre, 12 Union Road, Cambridge CB2 1EZ, UK; fax: (+44) 1223-336-033; or E-mail: deposit@ccdc.cam.ac.uk.

UV-vis absorption spectra was measured using a Shimadzu UV-3600 plus UV-vis-NIR spectrophotometer. The infrared spectra (4000~400cm^{-1}) were recorded on a NICOLET 6700 FT-IR spectrometer by incorporating the samples in KBr disks. Room temperature PL spectra and time-resolved lifetime were conducted on an Edinburgh FLS1000 fluorescence spectrometer equipped with a xenon arc lamp (Xe900) and nanosecond flash-lamp (nF900). Polarized fluorescence spectra of

DMP@**1** crystal sample were measured on Edinburgh FLS1000 fluorescence spectrometer by setting a polarizer in front of the detector. The crystal sample was irradiated by 500 nm, the polarization of the light signal can be obtained by rotating the polarizer at different polarization angle. ^{1}H-NMR spectra were recorded on a Bruker Advance II DMX 400 spectrometer with use of the deuterated solvent as the lock.

Optoelectronic performances were tested with a CHI 660E electrochemical analyzer (CH Instruments, Chenhua Co., Shanghai, China) in a standard three-electrode system. Ag/AgCl as a reference electrode, a platinum wire electrode as a counter electrode, powder of **1** and DMP@**1** modified indium tin oxide (ITO) as the working electrode (working area of 1.0 cm^2), and 0.5 M sodium sulfate aqueous solution as electrolyte. The system was irradiated by a 300 W Xe lamp. Transient photocurrent responses with the on–off cycle's illumination were tested in three-electrode system at ambient pressure and room temperature without bias potential.

2. Synthesis of $[(HOEtMIm)_2][Mn_3(TBAPy)_2(H_2O)_4]$ (1).

$Mn(Ac)_2$ (0.2 mmol) and H_4TBAPy (0.05 mmol) were soaked in 1 mL 1-(2-hydroxyethyl)-3-methylimidazolium chloride ([HOEtMIm]Cl) ionic liquid in a glass vial (10 mL), which was heated in an isotherm oven more than 100 °C until starting materials dissolved. 4 mL mixed solvent of DMF and H_2O (V/V = 1:1) was added, and then the homogeneous phase was transferred to a 25 mL Teflon-lined stainless steel vessel. The vessel was sealed and heated to 160 °C for 72 h and then cooled to room temperature at a rate of 5 °C·h^{-1}. Pale yellow block crystals of **1** were obtained in high yields (~90%).

3. Synthesis of DMP@1

50 mg of crystal samples of **1** were immersed into the EtOH solution (10 mL) of 2-[4-(Dimethylamino)styryl]-1-methylpyridinium iodide (3×10^{-4} mg/L) at ambient temperature for 3 days in darkness. Subsequently, the resulting samples were filtered off, washed several times with EtOH and then dried in air.

4. Preparation of working electrode.

The indium tin oxide (ITO) substrate (1 × 4 cm^2) was firstly washed by ethanol, and water under ultrasonic processing for about 30 min then dried in natural environment. Powder of **1** or DMP@**1** (20 mg) was added into 0.5 mL anhydrous ethanol, then ultrasonicated for 30 min to form suspension liquid. The working electrodes were prepared by dropping the above suspension (0.2 mL) onto the surface of the pre-treated ITO by controlling the coating area about 1 cm^2, and allowing it to dry at room temperature.

5. Theoretical calculations.

The density functional theory (DFT) calculations were performed by Material Studio software package[3] Dmol[3] module.[4] Both of free H_4TBAPy and H_4TBAPy dimer for DFT calculations were obtained by removing the symmetry of the crystallographic information file (cif) of the MOF. Perdew-Wang (PW91)[5] generalized gradient approximation (GGA) method was used for the full optimization of initial configuration. The self-consistent field (SCF) converged criterion was within 1.0 × 10^{-5} hartree $atom^{-1}$ and the converging criterion of the structure optimization was 1.0 × 10^{-3} hartree $bohr^{-1}$.

B. Supporting Figures

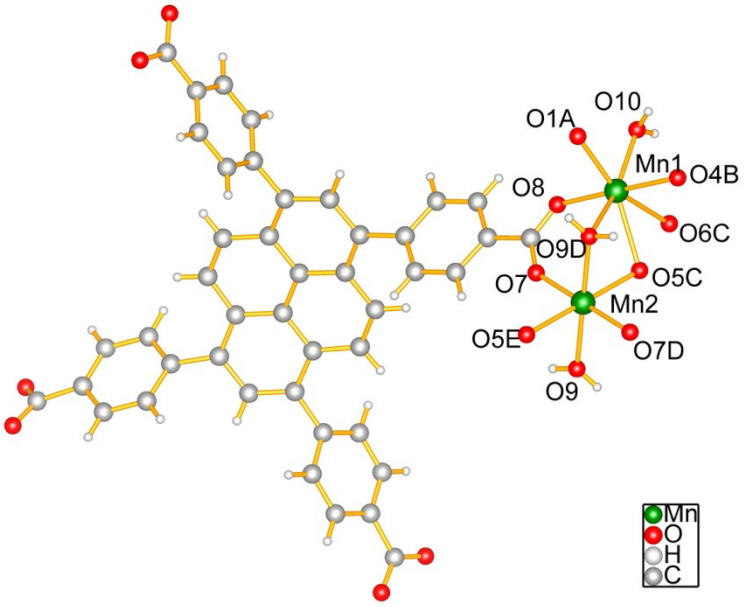

(a)

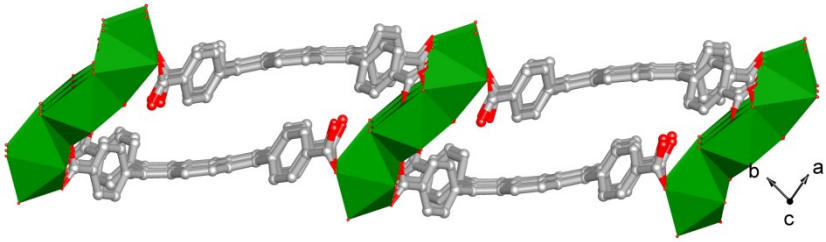

(b)

Figure S1. (a) View of local coordination environment of Mn(II) ion in **1**. Symmetry codes: A = -1+ *x*, 1+ *y*, + *z*; B = -1+X, 1+ *y*, -1+ *z*; C = + *x*, + *y*, -1+ *z*; D = 1- *x*, 2- *y*, - *z*; E = 1- *x*, 2- *y*, 1- *z*. (b) View of the 2D anionic double layer structure of **1** along *c* direction.

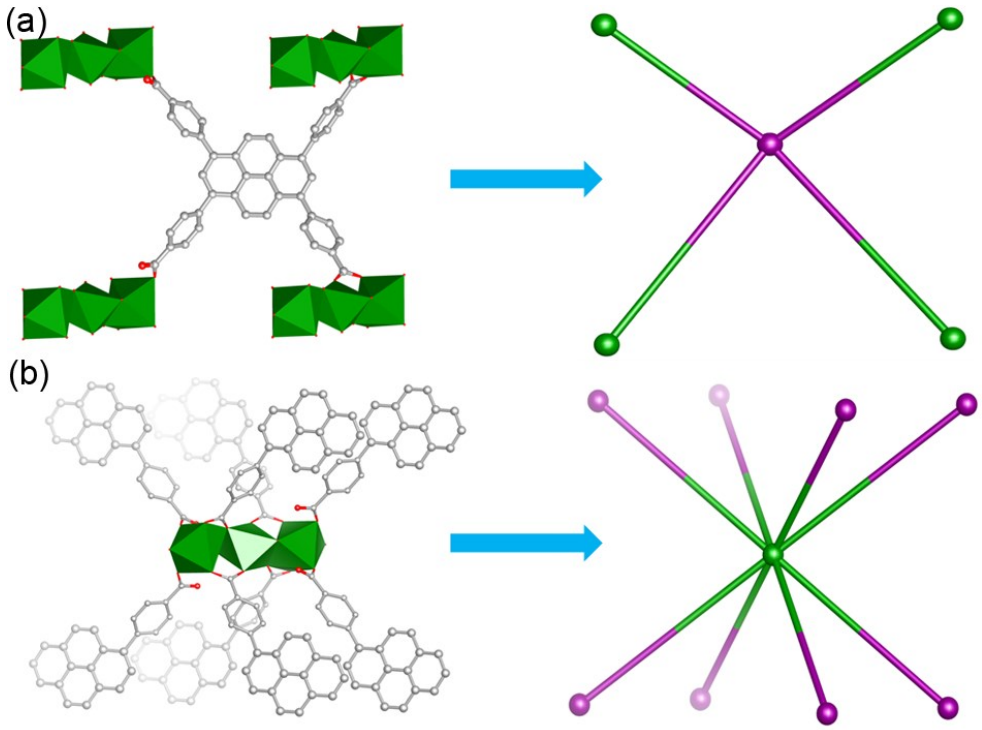

Figure S2. Schematic representation of 4-connected TBAPy node (a) and 8-connected $\{Mn_3\}$ cluster (b) in **1**.

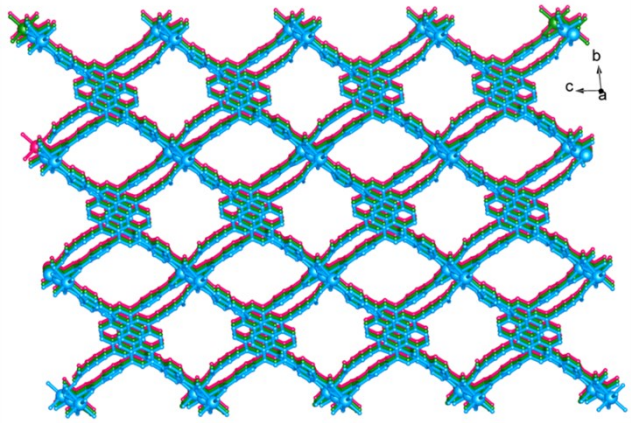

(a)

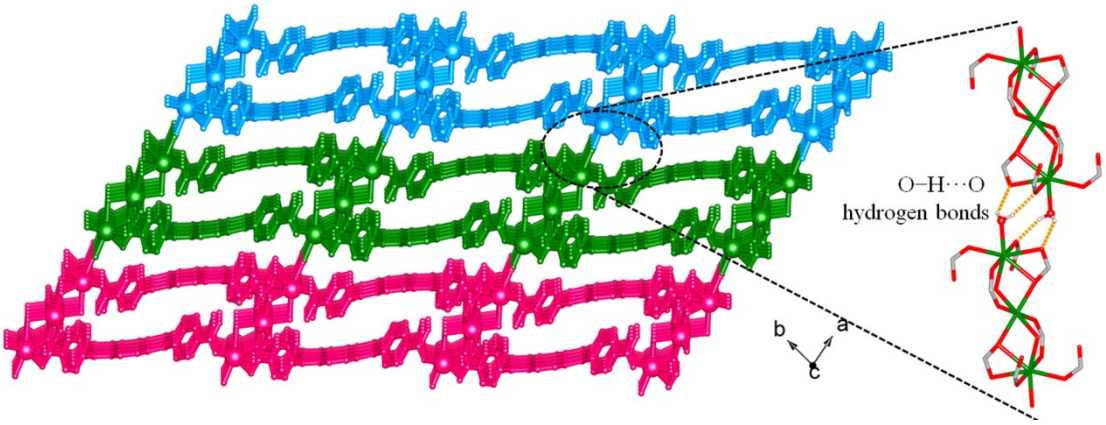

(b)

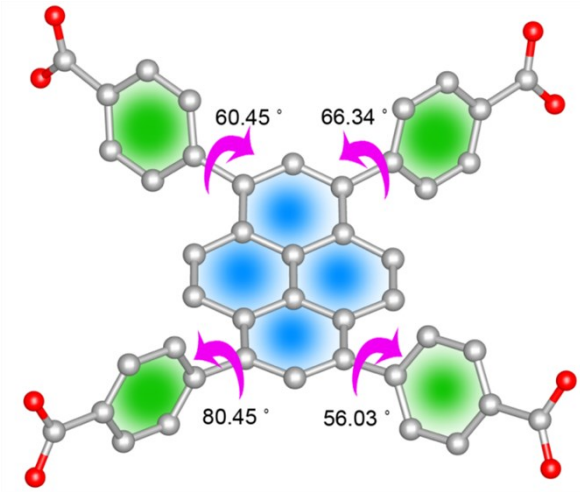

(c)

Figure S3. View of the 3D stacking structure of **1** along *a* (b) and *c* (b) direction extended by O−H···O hydrogen bonds between the terminal coordinated water molecules and carboxylate groups. Layers show different color for clarity. (c) Dihedral angles between the central pyrene core and four benzoate motifs in **1**.

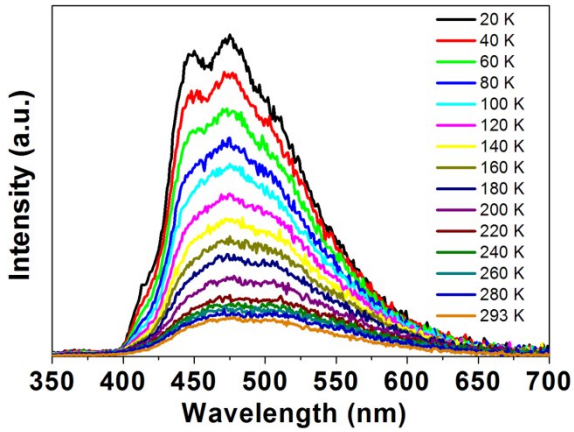

(a)

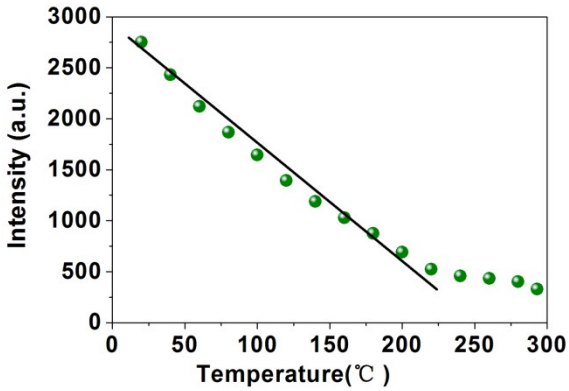

(b)

Figure S4. (a) Steady-state fluorescence spectra of **1** measured at temperatures from 293 to 20 K. (b) The temperature-dependent fluorescence intensities.

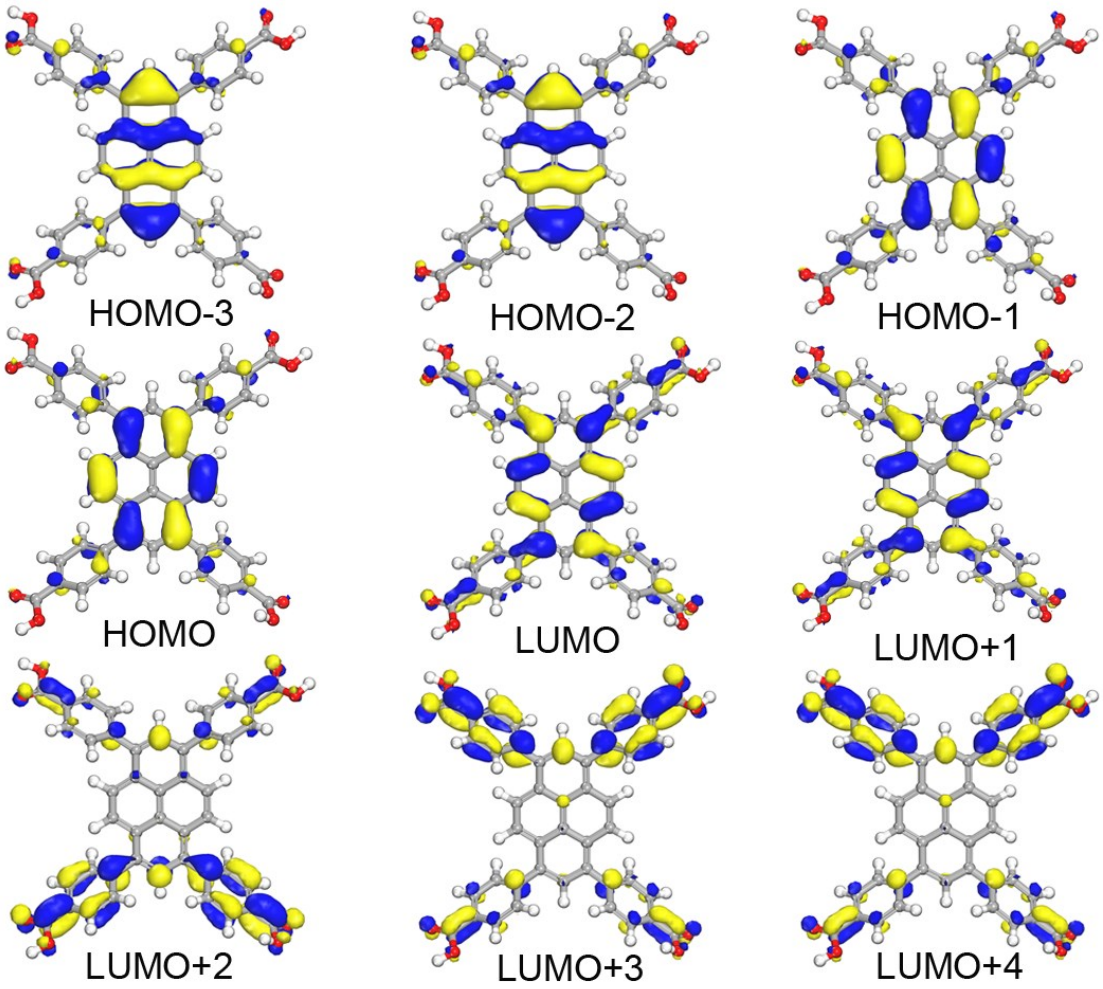

Figure S5. View of HOMOs and LUMOs for the DFT optimized structure of free H_4TBAPy.

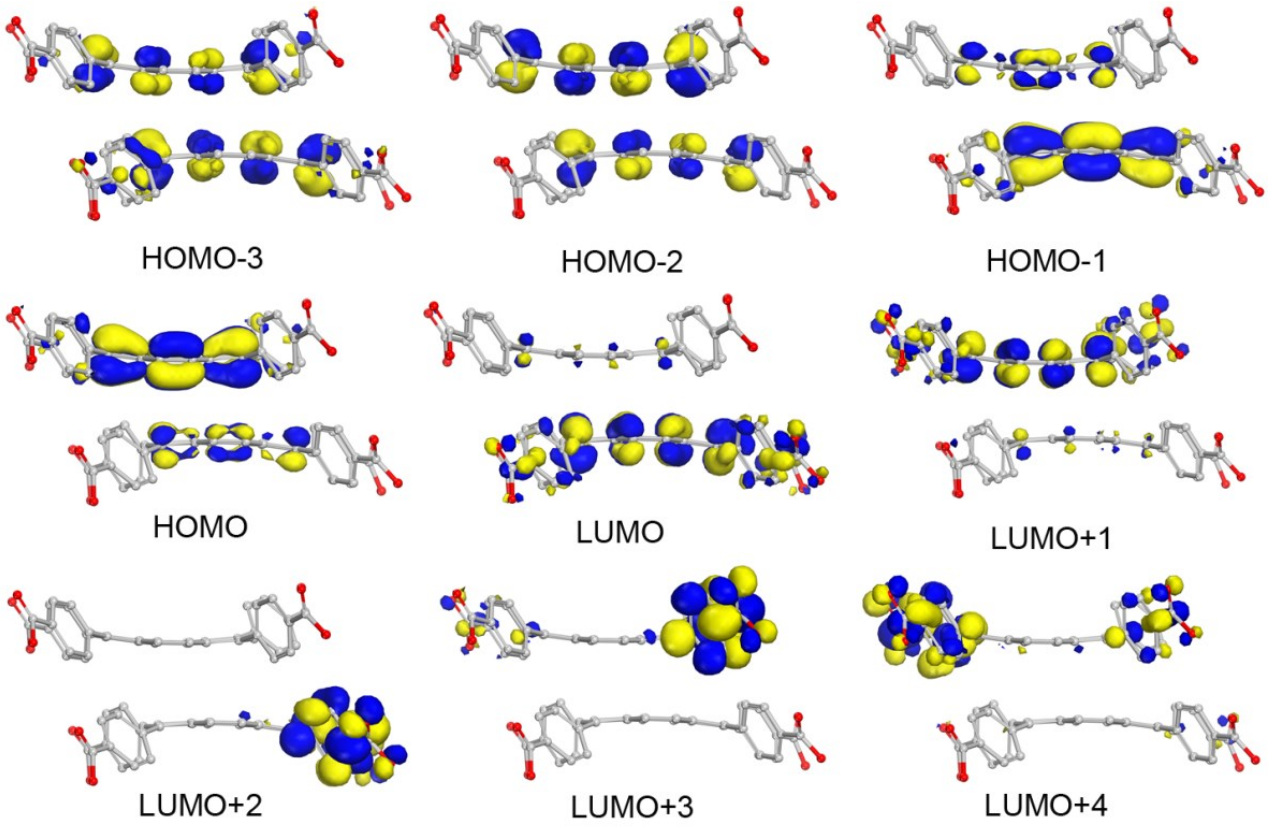

Figure S6. View of HOMOs and LUMOs for the DFT optimized structure of H_4TBAPy dimer in **1**.

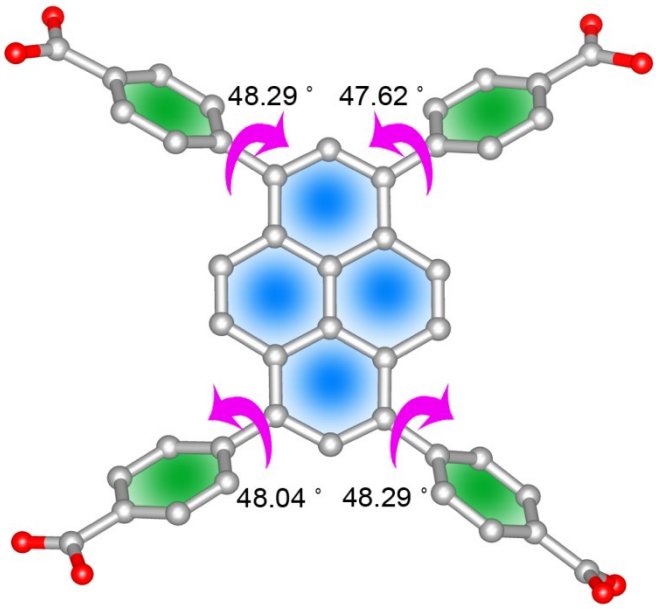

Figure S7. Dihedral angles between the central pyrene core and four benzoate motifs calculated from the simulated free H_4TBAPy.

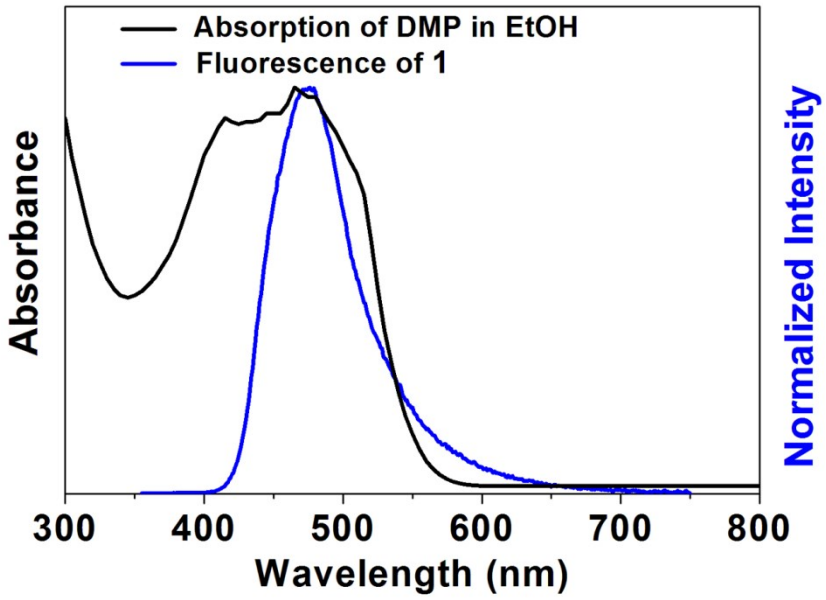

Figure S8. Normalized UV-vis absorption of DMP and fluorescence spectra of **1**. The absorption spectra of free DMP was measured in EtOH.

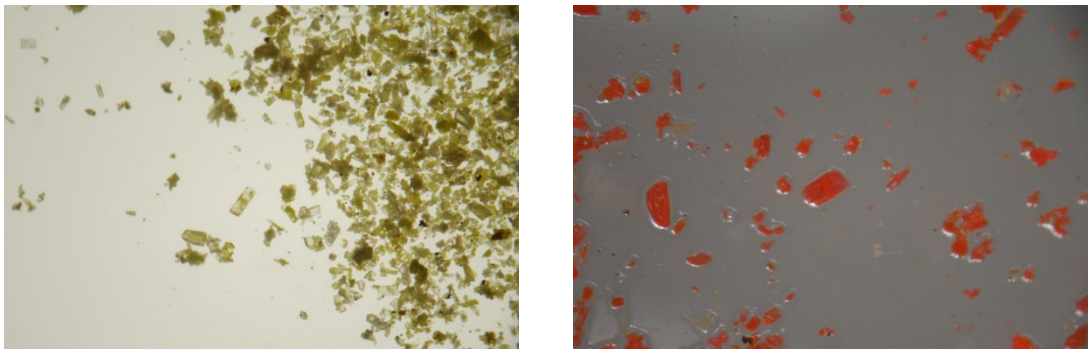

(a) (b)

Figure S9. Digital photographs of single crystals of **1** (a) and DMP@**1** (b).

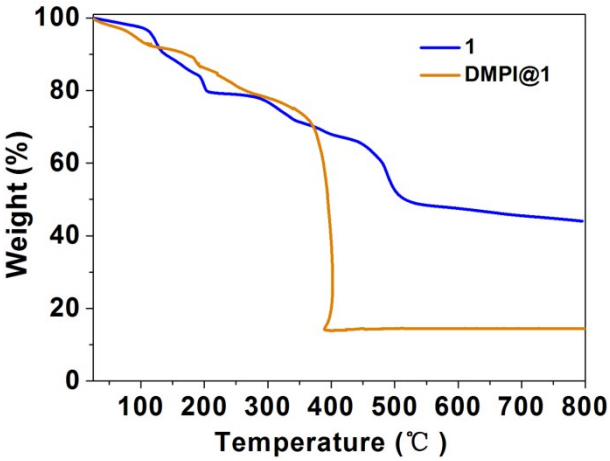

(a)

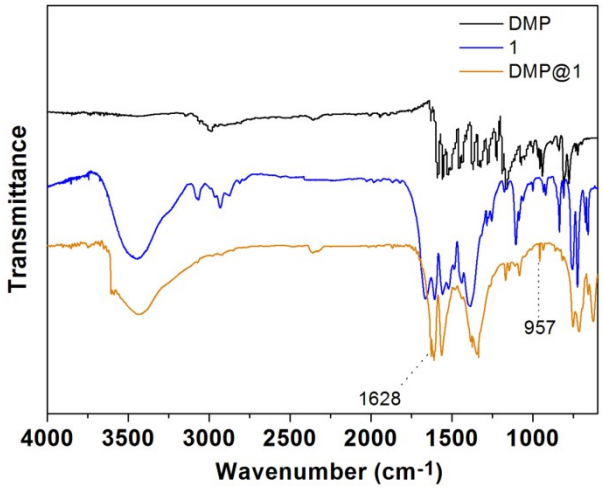

(b)

Figure S10. Thermogravimetric curves (a) and FT-IR spectra of (b) **1** and DMP@**1**. The obtained band at about 1628 and 957 cm^{-1} can be assigned to the characteristic absorption peak of the C=C and pyridinium ring for DMP, respectively.

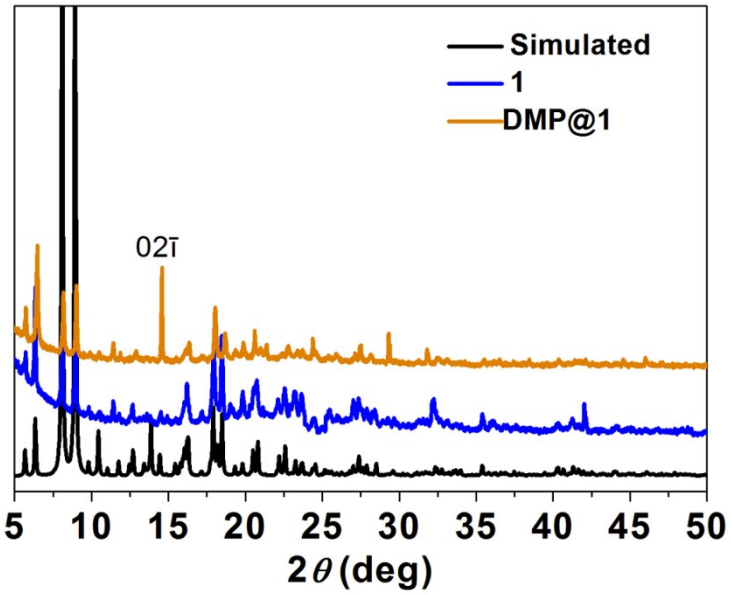

Figure S11. PXRD patterns of **1** and DMP@**1**.

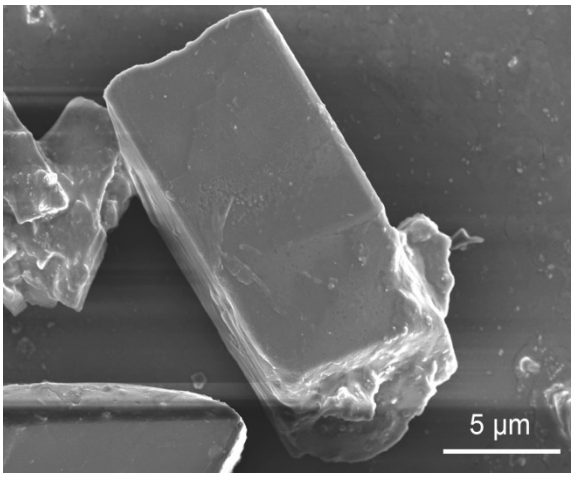

(a)

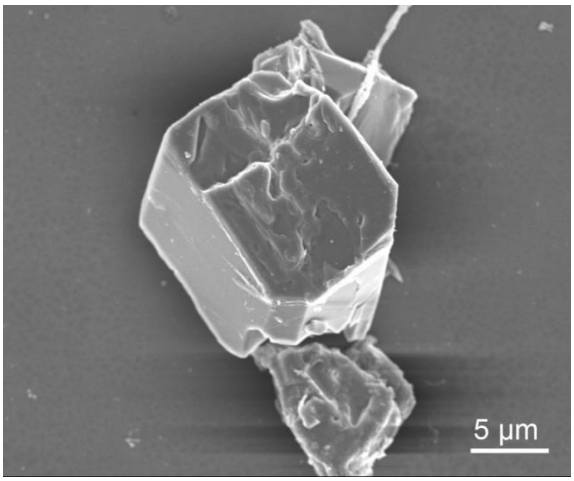

(b)

Figure S12. SEM images of **1** (a) and DMP@**1** (b) bulk crystals.

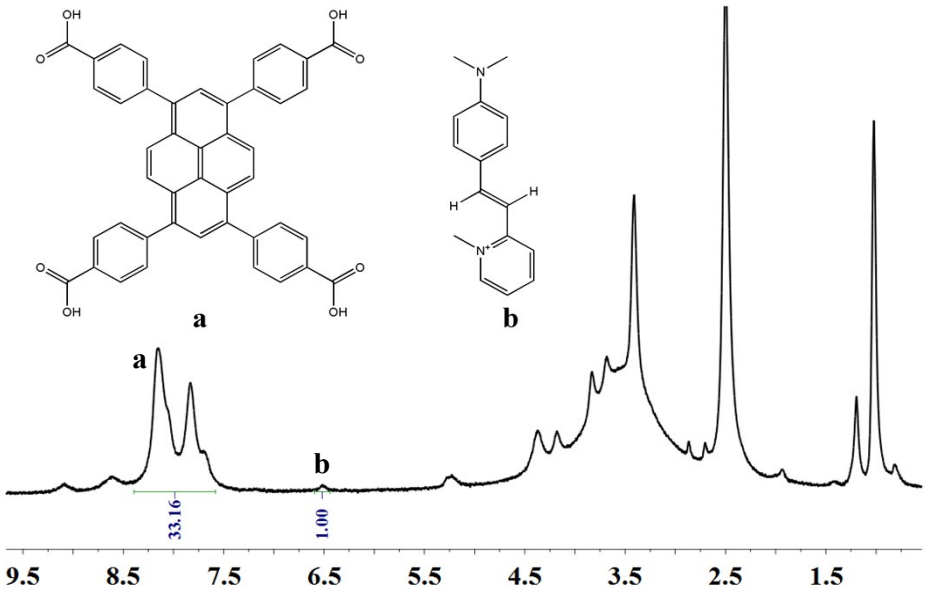

Figure S13. ^{1}H-NMR spectra (400 MHz) of **DMP@1** dissolved in DCl, D_2O, and DMSO-d_6. The ratio of DMP to TBAPy ligand in DMP@**1** was calculated as about 1:9. Thus, the chemical formula of DMP@**1** can be labeled as $[(HOEtMIm)_{16/9}(DMP)_{2/9}][Mn_3(TBAPy)_2(\mu_2\text{-}OH_2)_2(H_2O)_2]$ (**1**).

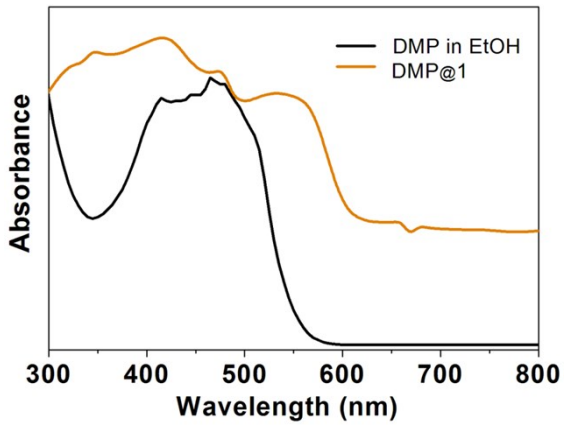

Figure S14. The UV-vis absorption of DMP and DMP@**1**. The absorption spectra of free DMP was measured in EtOH.

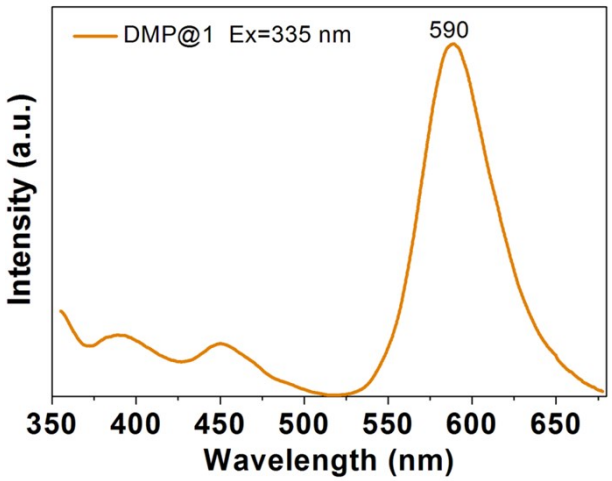

Figure S15. The fluorescence spectra of DMP@**1** excited by 335 nm.

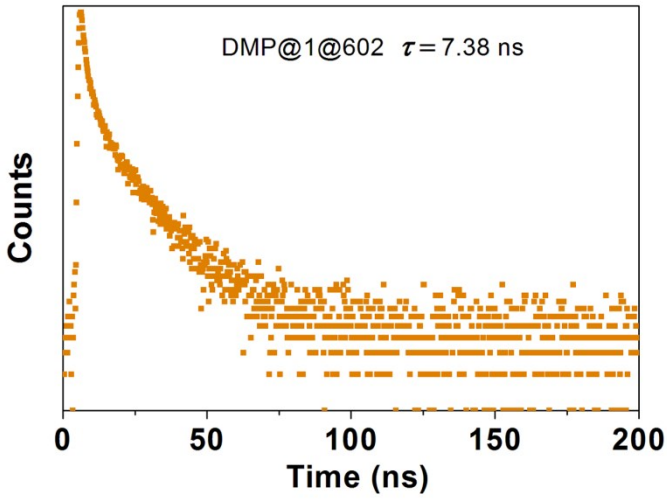

Figure S16. Fluorescence decay curve of DMP@**1** measured at room temperature.

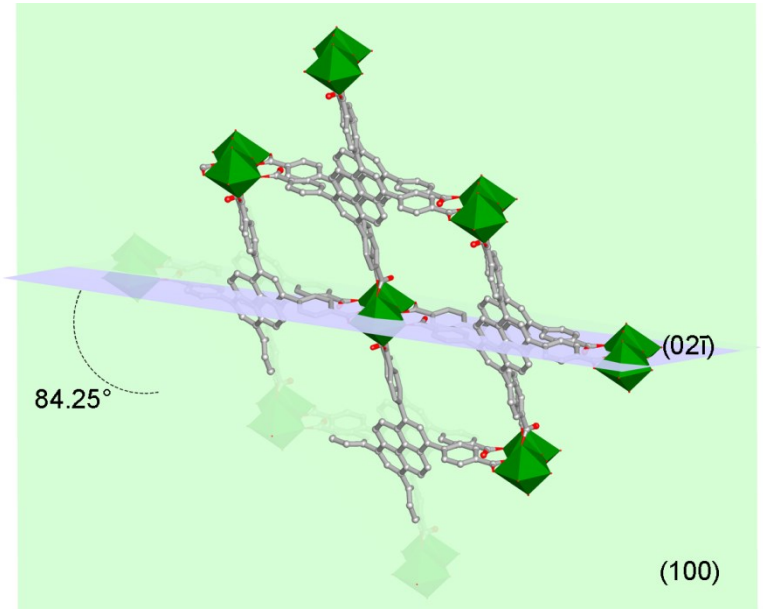

Figure S17. The dihedral angle between (02ī) and (100) platelet.

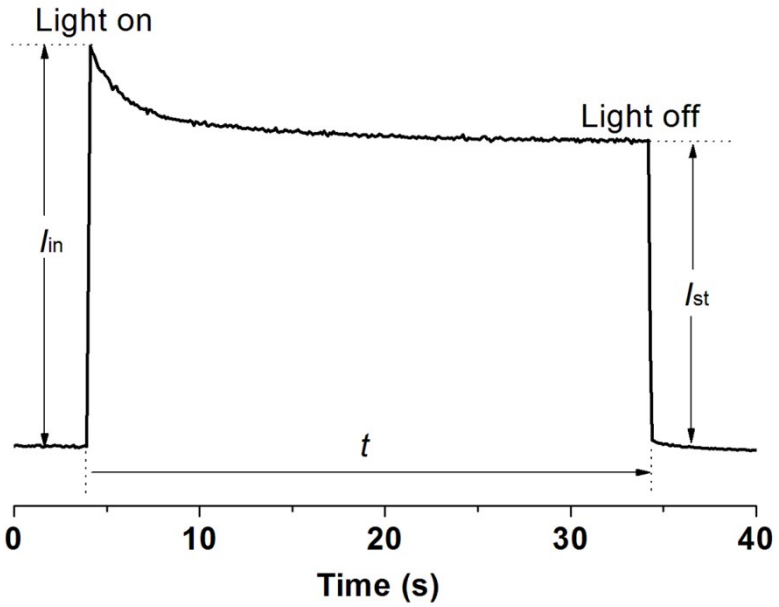

Figure S18. The typical transient photoresponse of the photoelectrode.

C. Supporting Tables

Table S1. Crystallographic data and experimental details for **1**.

Complex	**1**
Empirical formula	$C_{100}H_{74}N_4Mn_3O_{22}$
Formula weight	1848.49
Temperature/K	286.43(14)
Crystal system	triclinic
Space group	$P\bar{1}$
a/Å	11.5063(4)
b/Å	14.2794(5)
c/Å	15.8755(5)
α/°	82.493(3)
β/°	79.885(3)
γ/°	78.397(3)
Volume/Å^3	2503.06(15)
Z	1
ρ_{calc}g/cm^3	1.058
μ/mm^{-1}	0.430
F(000)	815.0
Crystal size/mm^3	0.24 × 0.22 × 0.2
Radiation	MoKα (λ = 0.71073)
Reflections collected	46113
Independent reflections	8652 [R_{int} = 0.0680, R_{sigma} = 0.0735]
Data/restraints/parameters	8652/0/502
Goodness-of-fit on F^2	1.060
Final R indexes [I>=2σ (I)]	R_1 = 0.0552, wR_2 = 0.1314
Final R indexes [all data]	R_1 = 0.0823, wR_2 = 0.1393
Largest diff. peak/hole / e Å^{-3}	0.36/-0.25

[a] $R = [\sum ||F_0| - |F_c|| / \sum |F_0|]$, $R_W = \sum_W [|F_0^2 - Fc^2|^2 / \sum_W (|F_w|^2)^2]^{1/2}$

Table S2. Selected bond distances /Å and bond angles /° for **1**.

Mn1- O1[1]	2.208(2)	Mn2- O5[5]	2.194(2)
Mn1- O4[2]	2.201(2)	Mn2- O5[3]	2.194(2)
Mn1- O5[3]	2.429(3)	Mn2- O7[4]	2.092(2)
Mn1- O6[3]	2.473(3)	Mn2- O7	2.092(2)
Mn1- O8	2.146(2)	Mn2- O9[4]	2.169(2)
Mn1- O9[4]	2.411(2)	Mn2-O9	2.169(2)
Mn1- O10	2.213(2)		
O1[1]-Mn1-O6[2]	156.25(9)	O10-Mn1-O6[2]	77.71(8)
O1[1]-Mn1-O9[3]	82.57(8)	O10-Mn1-O9[3]	159.38(8)
O1[1]-Mn1-O10	78.54(8)	O5[2]-Mn2-O5[5]	180.00(12)
O4[4]-Mn1-O1[1]	91.69(9)	O7[3]-Mn2-O5[2]	90.01(11)
O4[4]-Mn1-O5[2]	89.46(9)	O7-Mn2-O5[5]	90.01(11)
O4[4]-Mn1-O6[2]	86.30(8)	O7-Mn2-O5[2]	89.99(11)
O4[4]-Mn1-O9[3]	86.45(8)	O7[3]-Mn2-O5[5]	89.99(11)
O4[4]-Mn1-O10	85.93(8)	O7-Mn2-O7[3]	180.0
O5[2]-Mn1-O6[2]	52.74(8)	O7[3]-Mn2-O9[3]	91.75(10)
O8-Mn1-O1[1]	89.38(9)	O7-Mn2-O9[3]	88.25(10)
O8-Mn1-O4[4]	178.91(9)	O7-Mn2-O9	91.75(10)
O8-Mn1-O5[2]	89.69(9)	O7[3]-Mn2-O9	88.25(10)
O8-Mn1-O6[2]	92.64(9)	O9[3]-Mn2-O5[2]	77.33(9)
O8-Mn1-O9[3]	93.88(8)	O9-Mn2-O5[5]	77.33(9)
O8-Mn1-O10	94.10(8)	O9-Mn2-O5[2]	102.67(9)
O9[3]-Mn1-O5[2]	68.56(8)	O9[3]-Mn2-O5[5]	102.67(9)
O9[3]-Mn1-O6[2]	120.84(8)	O9[3]-Mn2-O9	180.
O10-Mn1-O5[2]	130.44(8)		

Symmetry operations: [1]-1+X,1+Y,+Z; [2]+X,+Y,-1+Z; [3]1-X,2-Y,-Z; [4]-1+X,1+Y,-1+Z; [5]1-X,2-Y,1-Z.

D. Supporting References

[1] CrysAlisPro, Rigaku Oxford Diffraction, Version 1.171.39.6a.

[2] G. M. Sheldrick, *Acta Crystallogr. Sect. A* 2008, **64**, 112.

[3] (*a*) B. Delley, *J. Chem. Phys*. 1990, **92**, 508; (*b*) B. Delley, *J. Chem. Phys*. 2000, **113**, 7756.

[4] Dmol^3 Module, MS Modeling, Version 2.2; Accelrys Inc.: San, Diego, 2003.

[5] J. P. Perdew, J. A. Chevary, S. H. Vosko, K. A. Jackson, M. R. Pederson, D. J. Singh and C. Fiolhais, *Phys. Rev. B* 1992, **46**, 6671.